Ribbon Formation in Twist-Nematic Elastomers

L. Teresi, V. Varano

LaMS - Modeling & Simulation Lab,
Università Roma Tre, Italy

COMSOL Conference Europe 2012, Milan, Italy
October, 10 ∼ 12, 2012

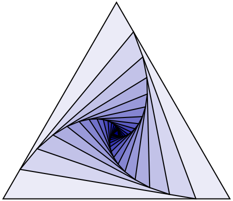

1. Helicoid to Ribbon

1.1 Formation of twisted ribbons consisting of bilayers of gemini surfactants (two surfactant molecules covalently linked at their charged head groups; here 16-2-16 tartrate at 0.1% in water; horizontal span $\sim 10\,\mu m$).

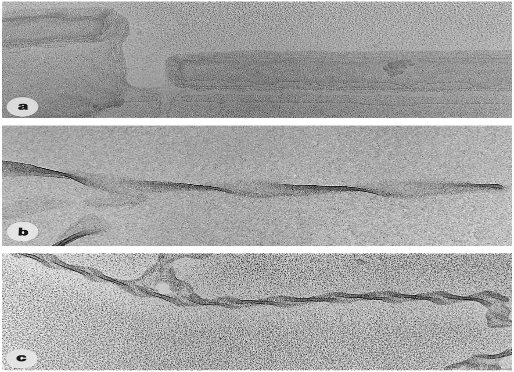

R. Oda, I. Huc, M. Schmutz, S.J. Candau, F.C. MacKintosh.
Tuning bilayer twist using chiral counterions. NATURE, vol. 399, 1999.

1.2 It is observed a smooth transition from platelet to helix to ribbon (tubule in the picture)

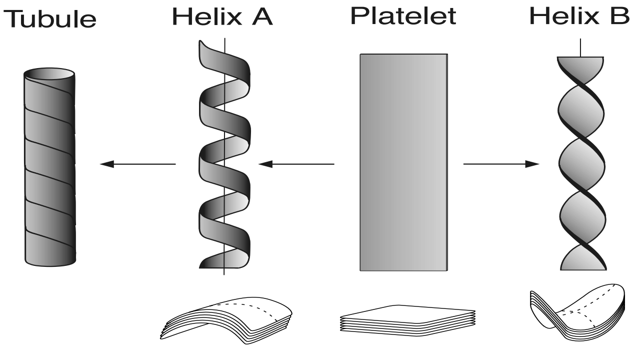

1.3 How does the shape of the twisted ribbons arise from the particular molecular structure of the amphiphiles?

R. Oda, I. Huc, M. Schmutz, S.J. Candau, F.C. MacKintosh.
Tuning bilayer twist using chiral counterions.
NATURE, vol. 399, 1999.

1.4 This is a long lasting story ...

W. Helfrich, J. Prost.
Intrinsic bending force in anisotropic membranes made of chiral molecules.
Physical Review A, vol. 38, n. 6, 1998.

R. Oda, I. Huc, M. Schmutz, S.J. Candau, F.C. MacKintosh.
Tuning bilayer twist using chiral counterions.
NATURE, vol. 399, 1999.

R. Ghafouri, R. Bruinsma.
Helicoid to Spiral Ribbon Transition.
Physical Review Letters, vol. 94, 2005.

E. Efrati, E. Sharon, R.Kupferman.
Buckling transition and boundary layer in non-Euclidean plates.
Physical Review E, vol. 80, 2009.

Y. Sawaa, F. Ye, K. Urayama, T. Takigawa, V. Gimenez-Pinto, R.L.B. Selinger, J.V. Selinger,
Shape selection of twist-nematic-elastomer ribbons.
PNAS, vol. 108, n. 16, 2011.

1.5 ... and here is what happens to Twist-Nematic Elastomers

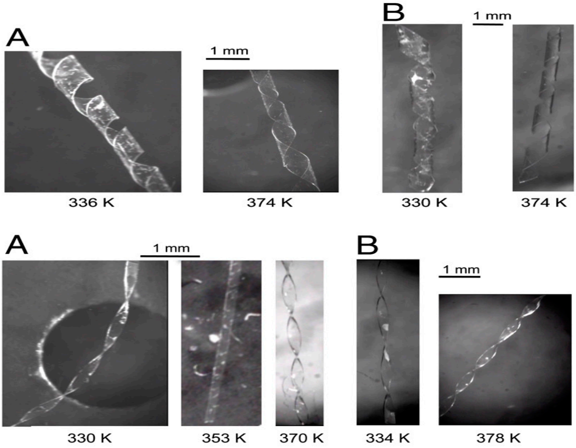

Y. Sawaa, F. Ye, K. Urayama, T. Takigawa, V. Gimenez-Pinto, R.L.B. Selinger, J.V. Selinger,
Shape selection of twist-nematic-elastomer ribbons.
PNAS, vol. 108, n. 16, 2011.

2.1 Nematic elastomers exhibit large distortions of a special kind:

if the stress-free shape of a mesoscopic chunk of NE is a spherical ball when the appended mesogens are in the disordered, isotropic phase (left), its stress-free shape in the ordered, nematic phase is a spheroid whose polar axis is aligned with the prevailing mesogen direction (right).

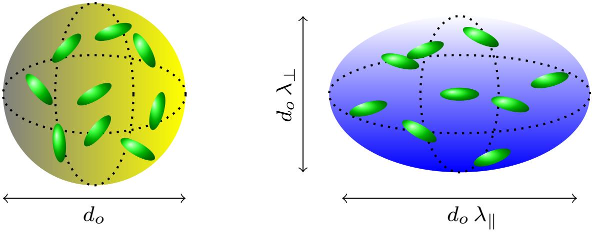

Isotropic phase

Nematic phase

3. Isotropic-nematic Phase Transitions

3.1 Nematic direction is represented by

$$\mathbf{N} = \mathbf{n} \otimes \mathbf{n}\,, \quad \text{with } \mathbf{n} \text{ a unit vector, called } \textbf{director}$$

3.2 Nematic distortions are then represented by the tensor

$$\mathbf{U}_o = \lambda_\parallel \, \mathbf{N} + \lambda_\perp \, (\mathbf{I} - \mathbf{N})\,, \quad \lambda_\perp = \sqrt{\frac{J_o}{\lambda_\parallel}}\,, \quad J_o = \det(\mathbf{U}_o)$$

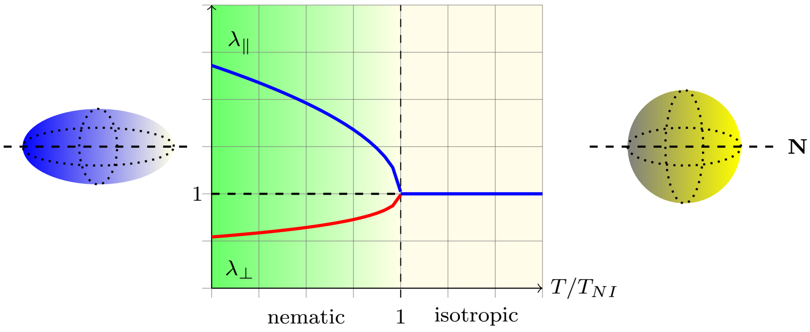

Phase diagram of a typical NE: strains versus temperature ($J_o = 1$).

4.1 Given a volume element dV, the elastic deformation $\mathbf{F}_e$ measures the difference between its distorted image $dv_o = \mathbf{U}_o\, dV$ and its actual state $dv = \mathbf{F}\, dV$.

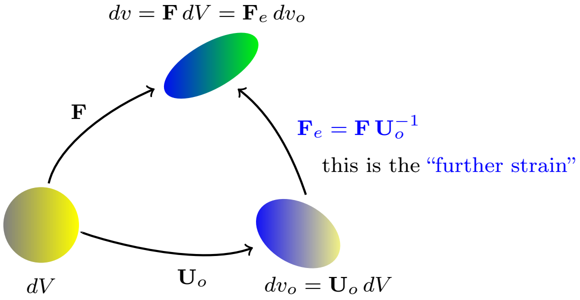

4.2 The elastic energy φ has to be a function of the elastic strain $\mathbf{C}_e = \mathbf{F}_e^{\top}\mathbf{F}_e$:

Y. Sawaa, K. Urayama, T. Takigawa, A. DeSimone, L. Teresi, **Thermally Driven Giant Bending of Liquid Crystal Elastomer Films with Hybrid Alignment**, Macromolecules, 2010.

5. Preparation

5.1 Specimens are prepared in the nematic & wet state, and are initially flat. The nematic configuration is imprinted in the elastomer matrix by the cross-linking reaction in the presence of a nonreactive dopant, and appropriate glass substrates coated with uniaxially rubbed layer.

5.2 The specimen undergoes an **anisotropic de-swelling** (irreversible) and a temperature-controlled nematic-to-isotropic phase transition (reversible)

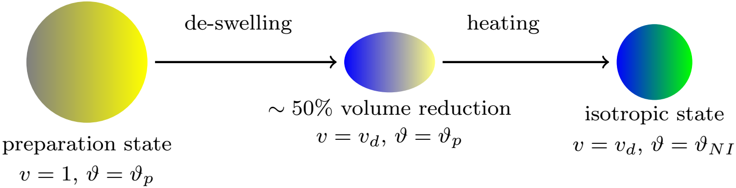

5.3 Nematic distortions are then represented by the tensor

$$\mathbf{U}_o = \frac{\lambda_{\|}(\vartheta)\,\alpha_{\|}(v)}{\lambda_{\|}(\vartheta_p)}\,\mathbf{N} + \frac{\lambda_{\perp}(\vartheta)\,\alpha_{\perp}(v)}{\lambda_{\perp}|(\vartheta_p)}\,(\mathbf{I} - \mathbf{N})\,.$$

5.4 Nematic-isotropic transition is volume preserving, de-swelling is not:

$$\lambda\|(\vartheta)\,\lambda_\perp^2(\vartheta) = 1\,, \quad \alpha\|(v)\,\alpha_\perp^2(v) = v\,.$$

5.5 Let us have a look at the resultant strains:

$$\lambda_\|(\vartheta, v) = \frac{\lambda_\|(\vartheta)\,\alpha_\|(v_d)}{\lambda_\|(\vartheta_p)}\,, \quad \lambda_\perp(\vartheta, v) = \frac{\lambda_\perp(\vartheta)\,\alpha_\perp(v_d)}{\lambda_\perp|(\vartheta_p)}\,.$$

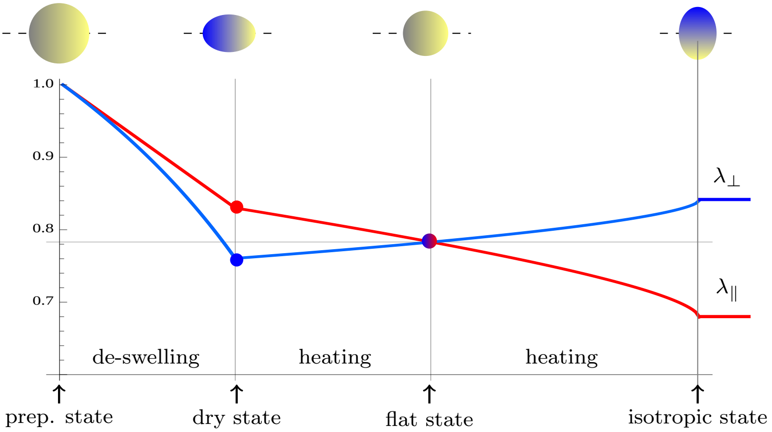

6. Chiral

6.1 Chiral geometry: $\mathbf{N}$ is on horizontal planes

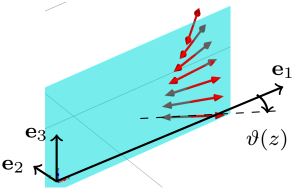

$$\vartheta = \vartheta(z)$$

$$\mathbf{n}(\vartheta) = \cos(\vartheta)\,\mathbf{e}_1 + \sin(\vartheta)\,\mathbf{e}_2$$

$$\mathbf{N}(\vartheta) = \mathbf{n}(\vartheta) \otimes \mathbf{n}(\vartheta)$$

$$\mathbf{U}_o(\vartheta) = \lambda_{\|}\,\mathbf{N}(\vartheta) + \lambda_{\perp}\,(\mathbf{I} - \mathbf{N}(\vartheta))$$

$$\mathbf{C}_o(\vartheta) = \lambda_{\|}^2\,\mathbf{N}(\vartheta) + \lambda_{\perp}^2\,(\mathbf{I} - \mathbf{N}(\vartheta))$$

6.2 What is the realized configuration?

6.3 The elastic strain must accommodate non-homogeneous and non isotropic distortions; we study two chiral geometries:

L-geom: at midplane director $\parallel$ axis

S-geom: at midplane director $\perp$ axis

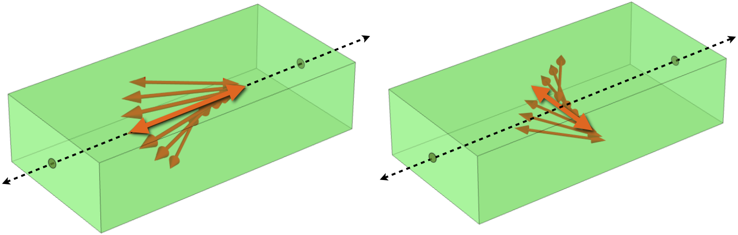

6.4 There are two strategies: twist or bend; the transition from one shape to the other is sharp.

7.1 The handedness is determined by the torsion b_{o12}:

$$b_{o12} > 0 \Rightarrow \quad \text{right-handed;} \qquad b_{o12} < 0 \Rightarrow \quad \text{left-handed.}$$

$$b_{o12} = \begin{cases} \frac{1}{2}(\lambda_{\parallel}^2 - \lambda_{\perp}^2) & \text{L-geometry;} \\ \frac{1}{2}(\lambda_{\perp}^2 - \lambda_{\parallel}^2) & \text{S-geometry.} \end{cases}$$

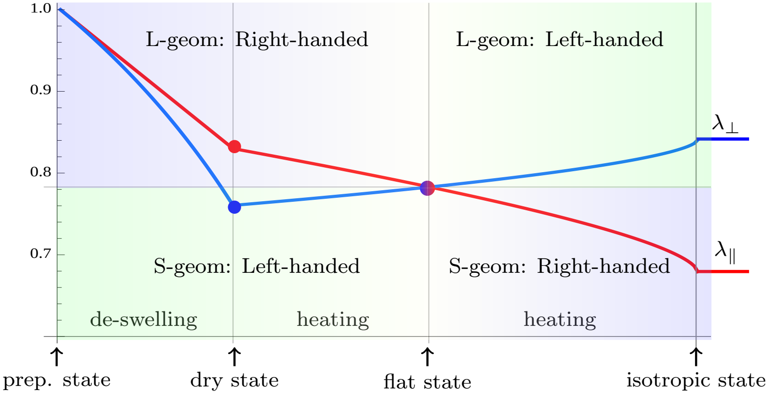

7.2 Helicoid to Ribbon

⇓ smooth transition

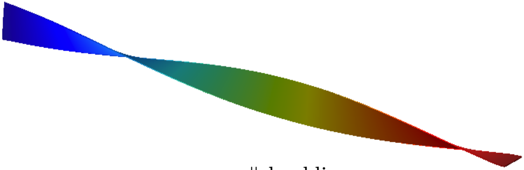

⇓ buckling

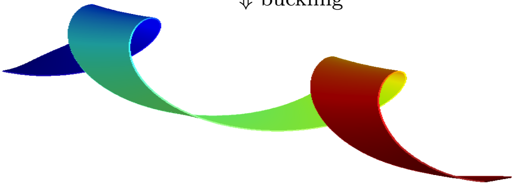

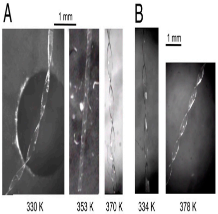

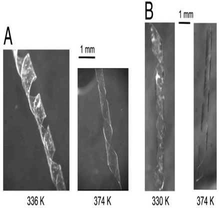

Y. Sawaa, F. Ye, K. Urayama, T. Takigawa, V. Gimenez-Pinto, R.L.B. Selinger, J.V. Selinger, **Shape selection of twist-nematic-elastomer ribbons**, PNAS, 2011.

8.1 Shape transition is dependent on the the ratio:

$$\frac{\text{torsional stiffness}}{\text{bending stiffness}} \propto \frac{\text{width}}{\text{height}}$$

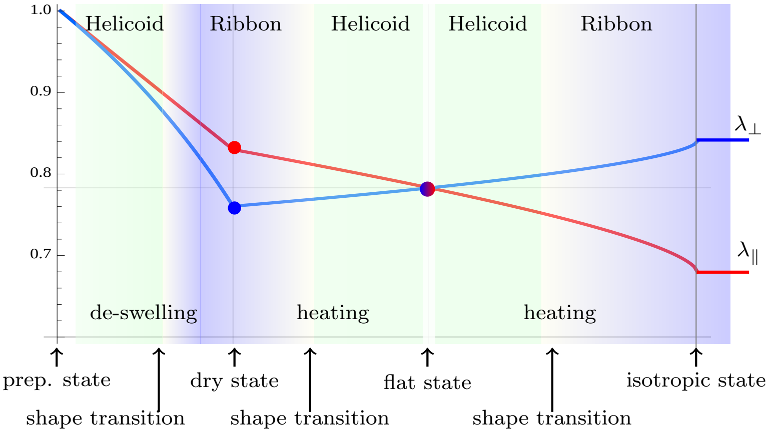

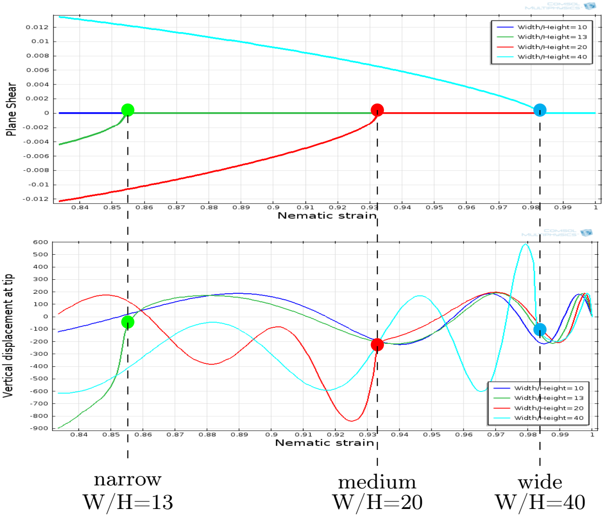
Width/Height=10
Width/Height=13
Width/Height=20
Width/Height=40
Plane Shear
Nematic strain
Vertical displacement at tip
Nematic strain
narrow
W/H=13
medium
W/H=20
wide
W/H=40

9.1 Narrow VS Wide bars

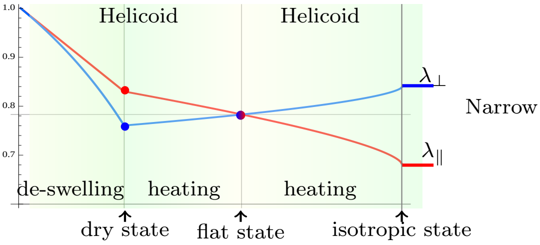

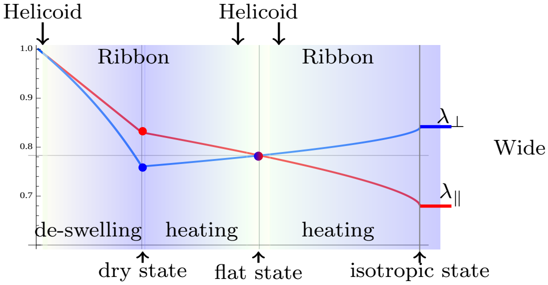

Acknowledgements

Kenji Urayama, Department of Materials Chemistry, Kyoto University, Japan, for having introduced me into the phenomenology of NEs, for many helpful discussions on the topic, and for sharing key experimental data.

Mathematics and Mechanics of Biological Assemblies and Soft Tissues, research grant sponsored by Italian Minister of University and Research, Italy.

Outstanding Paper Award by **Japanese Society of Liquid Crystals**

Y. Sawaa, K. Urayama, T. Takigawa, A. DeSimone, L. Teresi, **Thermally Driven Giant Bending of Liquid Crystal Elastomer Films with Hybrid Alignment**, Macromolecules, 2010.